

E020 INVERSION OF SBL DATA ACQUIRED IN SHALLOW WATERS

R. MITTET¹, L. LØSETH^{1,2}, S. ELLINGSRUD¹

¹EMGS, Stiklestadveien 1, Trondheim, N-7041, Norway

²Norwegian University of Science and Technology (NTNU)

Introduction

The Sea Bed Logging (SBL) method is described by Eidesmo et al. (2002). The main idea is to use an active source to probe the underground for thin high resistive layers. Hydrocarbon filled reservoirs will typically have a resistivity that is one to two orders of magnitude higher than a water filled reservoir. It will also have a resistivity that is one to two orders of magnitude higher than the surrounding shale or mudrock, and this is sufficient to support a partially guided wave that will leak energy up to receivers placed on the sea bed.

The actual experiment is performed by dropping electric and magnetic sensors on the sea bed along a predetermined sail line and thereafter towing a horizontal electric dipole along the line. The sail line starts at approximately 10 km before the first receiver on the line and ends at approximately 10 km after the last receiver. Thus, all receivers have at least active source data with source receiver offsets of ± 10 km. The situation where the boat is approaching a given receiver is called in-towing in the following. When the boat is leaving the same receiver, it is called out-towing.

Preprocessing

For the present dataset the source is towed 30 m above the seabed at 1.5 knots and emitting a square pulse with base frequency of 0.25 Hz. In the inversion we will use the contributions from the first, third and fifth harmonics, which are the three most energetic contributions. The modeling software used as engine in the inversion algorithm (Løseth, 2000) is a plane layer frequency-wavenumber algorithm. The modeling scheme includes the effect of the airwave. Hence, the airwave is naturally accounted for in the inversion scheme and need not be removed during the preprocessing stage. The modeling method describes a source placed at fixed offset, transmitting a harmonic signal, which in principle has infinite duration, so the modeled fields are not directly compatible with the acquired fields, which are from a moving source. The towing speed, however, is so low that for an interval of 30 to 40 periods, it can be viewed as located at a fixed source position. This argument is based on the long wavelengths, of order kilometers, that are typical for this experiment. The source will move less than one tenth of the shortest wavelength during 40 periods.

To convert the time-domain data to the frequency domain, we first decide on the number of source positions desired for the inversion. In this case we use 95 source positions at each side of the receiver. The first offset is 500 m and the last is 9900 m, thus, the distance between each source location is 100 m except for a 1 km gap at the receiver location. This area is avoided since it carries little or no information about any potential hydrocarbon reservoir and the measurements are also partly saturated close to the receiver. When the source positions are decided, we can map each source position, \vec{x}_s , to a time, T_s , based on the navigation. The transform from time to frequency domain for any of the two measured horizontal electric fields, E_i , is performed as follows,

$$E_i(\bar{x}_r, \omega | \bar{x}_s) = \frac{1}{\tau} e^{i\omega(T_s - \tau/2)} \int_0^{\tau} dt E_i(\bar{x}_r, t + T_s - \tau/2 | \bar{x}_s) e^{i\omega t} ,$$

where \bar{x}_r represents the receiver location. The transform interval, τ , is an integer number of periods, in the following 35 periods. At most locations the signal shows good repeatability within the transform interval. No tapering of the time domain signal is performed before the transformation. In this way, the frequency domain signal repeat itself also with a period of τ for infinite times and we have a measured field that is compatible with the modeled field. The phase factor in front of the integral is necessary to preserve phase and the division by the transform interval preserve amplitude/units.

Method

The inverse problem is non-unique and there will be many models that can explain the data, so constraints must be put on the allowed solution space. The strategy in this case has been to use depth converted seismic data to determine the layer geometry but let the resistivity in each layer be free to vary, as long as it is positive and above a certain lower level in the formation. The resistivity in the water layer is assumed known.

The error functional has the following form,

$$\varepsilon = \sum_{s, \omega, i} W(\bar{x}_s, \omega) \left[E_i^{data}(\bar{x}_s, \omega) - E_i^{mod}(\bar{x}_s, \omega) \right]^* \left[E_i^{data}(\bar{x}_s, \omega) - E_i^{mod}(\bar{x}_s, \omega) \right] .$$

The weigh factor, $W(\bar{x}_s)$, is the squared amplitude of the inline electric field for a low resistivity formation believed to be representative for the survey area. This behavior will balance the contributions from different offsets in the error functional. The field amplitudes are highly offset dependent, as are evident from the plot of the recorded data, shown in Figure 1. Figure 6 also indicate that noise becomes a problem for high offsets and high frequencies, so there is also a cutoff in the weight factor to avoid including these contribution in the optimization.

The sum over source positions goes over the in-towing part and the out-towing part of the experiment, however, one geological model is used for in-towing and another for out-towing. Since the underlying modeling scheme is a plane layer method, the method must be expected to work best in the case where the geology is plane layer on both sides of the receiver, however, it might be a reasonable approximation to a case where it is a change from one plane layer regime to another plane layer regime close to the receiver location.

The frequency summation is over the 3 most energetic contributions, resulting from the square source signal, that is the first, third and fifth harmonic. Tests on synthetic data revealed that for the presented method, at least the third harmonic was required to recover proper information below a high resistivity layer. It is also summed over the two polarizations of the electric field. When dropped, the receivers arrive at the seabed with an arbitrary orientation. A rotation to inline and crossline polarizations is performed on-the fly by having the rotation angle as one of the unknowns in the optimization problem. The system is driven by a Marquardt-Levenberg optimizer.

Results

Figure 1 show amplitude, and Figure 2 phase, of the acquired electric field for a receiver located at the known boundary of a hydrocarbon reservoir. The left side of each plot represent in-towing over an area without hydrocarbons and the right side represent out-towing over a hydrocarbon reservoir. There are strong relative amplitude contrasts as a function of offset on in-towing and out-towing, which are more obvious on Figure 3 where the synthetics (dashed line) are equal on both sides. The difference in phase, comparing in- and out-towing, is clearly seen in Figure 2.

The measured water depth at the location is 320 m, this is so shallow that we have a significant contribution from the airwave in the recorded data. The starting model has the true water depth, then follows interfaces at 420 m, 900 m, 1340 m, 1440 m and 3500 m, which is a crude representation of

the geology in the area. The resistivity is kept fixed at $0.32 \Omega m$ in the water layer. Initially the resistivity is set to $1 \Omega m$ in the rest of the formation, both on the in-towing and out-towing side. The comparison of the initial amplitude response and the data for the base frequency of 0.25 Hz is shown in Figure 3. The data is marked with a solid line and the modeled data with a dashed line. As can be expected, the initial model does not explain the data. In Figure 4 we show the same fields after the final iteration. The fit is clearly improved. In Figure 5, the result for the phase is shown. The difference on in-towing and out-towing is fairly well matched by the modeled data. Figure 6 include real (solid) and final synthetic data (dashed) for the 3 frequencies with the fifth harmonic as the lowest set. The higher harmonics are noisier, and below $10^{-9} V$ we approach the system noise level for the receiving antennas. Figure 7 show the final result. The model on the in-towing side is shown with a dashed line, the model on the out-towing side is shown with a solid line. The main goal is achieved, the non-hydrocarbon state is clearly separated from the hydrocarbon state. We note, however, that the model on the in-towing side show a resistivity between 900 m and the bottom of the reservoir that is probably too high. It is everywhere less than $10 \Omega m$, so it is not an indication of a high HC saturation and most probably due to limitations in the method or model geometry used here. On the out-towing side we note that the resistivity below the reservoir is unrealistically large. The last effect may be reduced with increased amplitude at high offsets on the higher harmonics. This is indicated by tests on synthetic data.

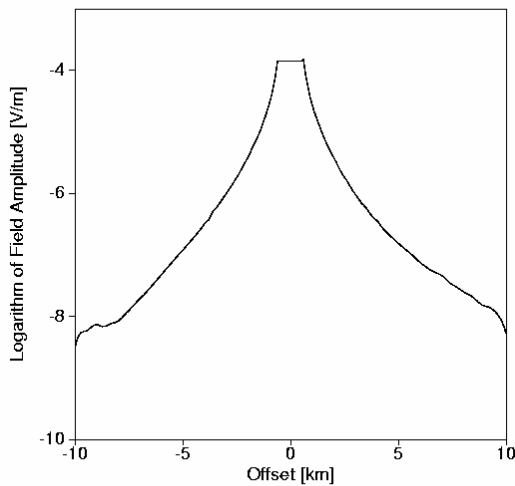


Fig. 1

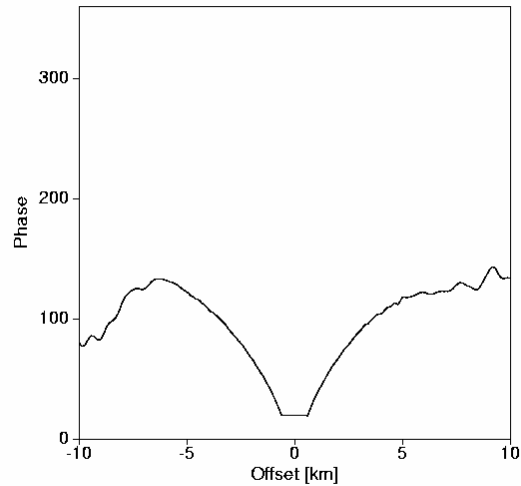


Fig. 2

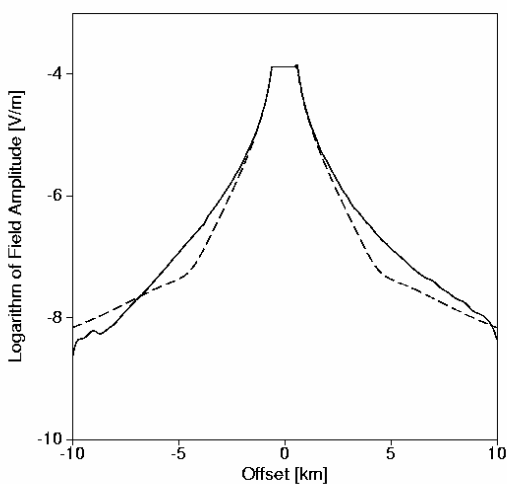


Fig. 3

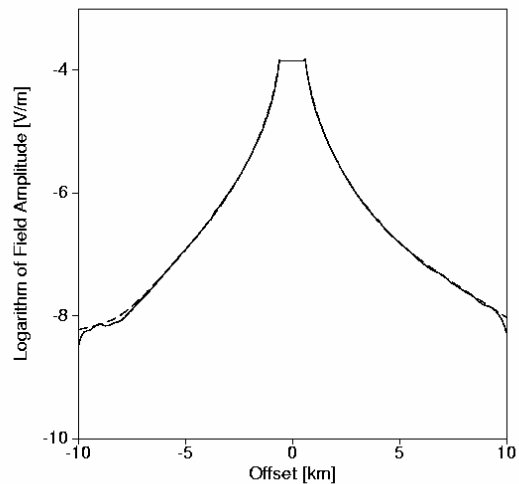


Fig. 4

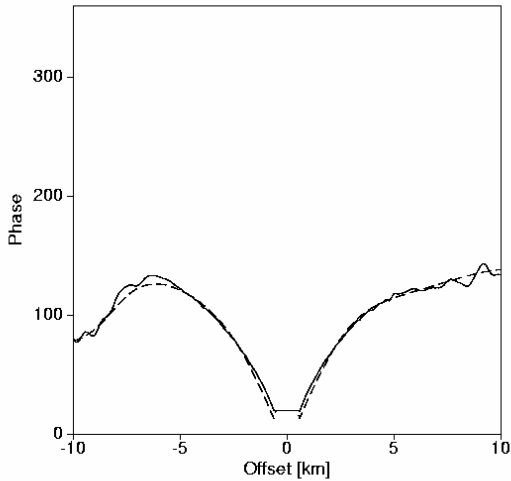


Fig. 5

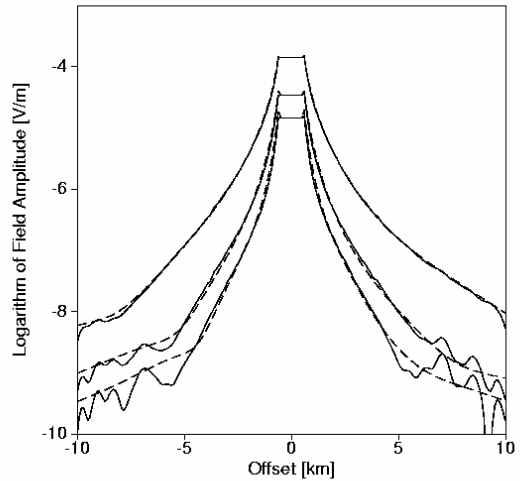


Fig. 6

Conclusion

Tests on noiseless synthetic data showed that additional frequencies to the first harmonic helped recovering low resistivity layers below high resistivity layers for SBL type data. A similar strategy was chosen for inversion of real data. Results from inversion of real data show a potential to separate the hydrocarbon from the non-hydrocarbon state with this method. Even if none of the two final models are exact, it is clear that the large contribution from the HC reservoir in the recorded data is reflected in the final resistivity model.

Both models have depths where we suspect the recovered resistivity to be too large. Some of these problems may be resolved by additional measurements. The method can be improved by inclusion of better constraints on the solution space and by introducing modeling schemes that handles lateral resistivity variations more consistently.

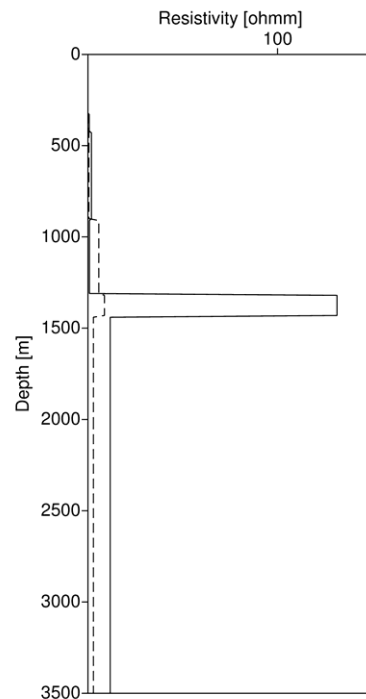


Fig. 7

References

Eidesmo, T., Ellingsrud, S., MacGregor, L.M., Constable, S., Sinha, M.C., Johansen, S., Kong, F.N., and Westerdahl, H., 2002, Sea Bed Logging (SBL), a new method for remote and direct identification of hydrocarbon filled layers in deepwater areas, *First Break*, 20,144-152

Løseth, L., 2000, Electromagnetic waves in layered media, M.Sc. thesis, NTNU.